LBWG memo 3

Definition of a coherent station in the pipeline

Neal Jackson, 2018.05.21, update**Testing of loop 3 on the 2015 test field data.**

2018.06.21

Summary. I examine various ways of characterising the coherence of visibilities on a particular station. The relevant quantity for our purposes is whether coherent phase calibration solutions can be obtained to that station, but this is not easy to measure without doing a phase calibration. The easy quantity to measure is the closure phase scatter between a station, ST001 and a nearby remote station. It is shown that, with an updated definition of the closure scatter, these correlate well and in practice a scatter of less than 0.80 in the closure phase statistic indicates that good solutions will be obtained. The updated closure phase statistic is calculated by version 4 of the closure.py script. Even this, however, does not give a robust statistic as it averages over multiple frequencies and is thus susceptible to delay errors. A method (implemented in version 5) gives a well-defined sigma for the overall detection of coherent signal.

1. Why do we care?

For any source that the pipeline is trying to calibrate on, or map, the source will have measurable structure on some baselines and not others. Nearly all sources have structure on scales of a few tens of kilometres, but experience with LBCS shows that structure becomes very much less bright on longer baselines as the source resolves out. Relatively few sources are still visible on 1000-km baselines.

We would like to know as early, and quickly, as possible in the pipeline process whether significant structure is present at particular spacings. There are three reasons for this:

- When deriving an initial model with the EHT imager, one needs to know which baselines have significant closure phase and which are likely to be noisy.
- When doing phase and delay solutions, it is useful to know which antennas to include. It is also useful to know what the coherence time is on particular antennas.
- It provides initial guidance on uv-tapers for imaging.

2. Closure phase scatter algorithm

One approach is to proceed regardless, and rely on identifying bad solutions after the event. This is likely to be highly wasteful. The alternative approach is to use closure phase. Typically one derives closure phase to an international station using ST001 and a relatively nearby remote station as the other two points of the closure triangle.

In general the closure statistic is formed using the empirically derived formula

```
np.nanmean(np.gradient(np.unwrap(cp))**2))
```

where `cp` is the closure phase derived from the closure triangle (in the range $-\pi \rightarrow \pi$). This statistic has a value of 1.64 for random noise, and zero for perfectly noiseless closure phases from a point source.

In versions up to v3 of the `closure.py` script, the algorithm simply consisted of reading in the data and applying this formula. There are two problems with the simplest version of the algorithm:

- The choice of threshold is arbitrary.
- The closure phase statistic depends on how far the data are averaged in time. (In practice one averages in frequency as much as possible, given the quality of the delay calibration). Averaging will give less scatter in general; however, if the averaging time exceeds the atmospheric coherence time, then the phases which make up the closure phase will begin to randomize.

3. Experiments with bright sources in the test field

The five brightest sources in the test field (Fig. 1) were used to test an updated closure algorithm. This algorithm calculates the closure statistic for a number of different averaging factors, from 8 seconds to 3 minutes. A polynomial was fit to the closure statistic and the minimum chosen. In some cases, particularly for the more resolved sources, the statistic does begin to increase as the averaging time increases. (Of course, one can use well-phase-calibrated data, in which case the problem will not arise).

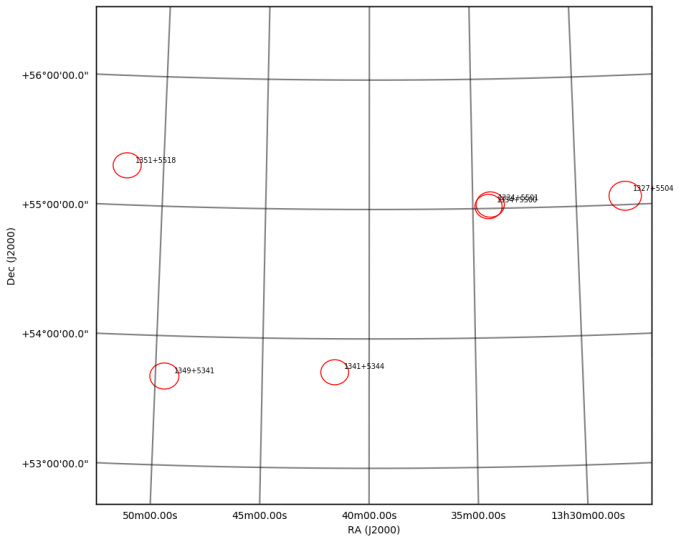

Figure 1: Bright sources in the test field

The phase dynamic spectra from baselines to ST001 were examined by eye for calibrated data on baselines from ST001 to international stations 601-608, and the results classified as coherent (P), not coherent (X) or just coherent in places (S):

	DE601	DE602	DE603	DE604	DE605	FR606	SE607	UK608
1327+5504	P	P	P	P	P	P	P	P
1334+5501	S	X	S	S	P	X	X	X
1341+5344	S	X	X	X	P	X	X	X
1349+5341	P	P	P	P	P	P	P	P
1351+5518	P	X	P	P	P	X	S	S

The closure phase statistics, updated as described and taken with ST001 and RS208 as the other corners of the triangle, are as follows:

	DE601	DE602	DE603	DE604	DE605	FR606	SE607	UK608
1327+5504	0.00	0.20	0.01	0.00	0.00	0.00	0.10	0.05
1334+5501	0.76	1.61	0.68	0.56	0.26	1.64	1.42	1.55
1341+5344	1.63	1.65	1.52	1.42	1.65	1.60	1.62	1.64
1349+5341	0.00	0.27	0.00	0.00	0.00	0.06	0.17	0.05
1351+5518	0.26	1.55	0.56	1.08	0.05	1.53	1.48	1.65

The statistic gives a good separation between eyeball judgements. In particular, all P baselines apart from one have values less than 0.60; S baselines range from 0.56 to 1.65; and X baselines are uniformly greater than 1.4.

Finally, we examine the extent to which phase selfcal solutions can be produced for different stations. This is probably the most important quantity, as it is directly related to whether that station can be used to image a particular source, or whether it will just contribute random noise. Since self-calibration is a global process, it may correlate imperfectly with the coherence of the source on the ST001 baseline.

Each source was selfcalibrated using CALIB in AIPS and the solutions were examined by eye. The quality of the solutions is rated from 1 to 4, where 1 means that all or nearly all solutions are coherent; 2 means significant gaps; 3 means partial, or mostly incorrect solutions; and 4 means few or no solutions. The results are as follows:

	DE601	DE602	DE603	DE604	DE605	FR606	SE607	UK608
1327+5504	1	1	1	1	1	1	1	1
1334+5501	1	2	1	1	1	4	4	4
1341+5344	4	4	4	4	4	4	4	4
1349+5341	1	1	1	1	1	1	2	1
1351+5518	2	4	3	4	1	4	4	4

These clearly correlate with the closure statistics on triangles involving the station together with ST001 and RS208. If the objective is to avoid bad solutions, it appears in practice that a cutoff of approximately 0.8 will do this.

4. A better way

In general, versions up to v4 of the closure phase script use only a fraction of the data. This is because only a few channels are typically used to derive the closure phase, for two reasons:

- If the delays have not been perfectly corrected, the phase on individual baselines – and hence the closure phase – will average to zero if a large bandwidth is used.
- The sources typically have structure which manifest as phase changes over a bandwidth of more than a few MHz. This also averages the closure phase to zero.

There is an algorithm which gets around both of those problems, while maintaining a better statistic for whether the source has been detected on a particular baseline. It also

rejects signal due to confusing sources in the field – which is very important if bright sources have not been perfectly subtracted.

One simply takes the dynamic closure phase spectrum (i.e. closure phase as a function of frequency and time) and Fourier transforms it. A major problem with this algorithm is edge effects; if there is bad data in a number of channels or at certain times, sharp edges cause ringing. This is avoided by replacing these areas by closure phases with random noise, at a small cost in signal-to-noise. Use of a control field of random phases also produces an estimate of the noise floor.

Fig. 2 shows this in practice. The triangle formed by the superterp, Effelsberg and Jülich is shown on the bright source 1327+5504. Coherent structure is obviously seen. It is measured by forming annuli around the central (zero-frequency) pixel and choosing the highest signal-to-noise annulus between 3 and 30 pixels around the centre (although this default can be changed). Such a maximum excludes fast-beating structure from external confusing sources, and the fact that a noise estimate is available means that the program gives a well-defined statistic.

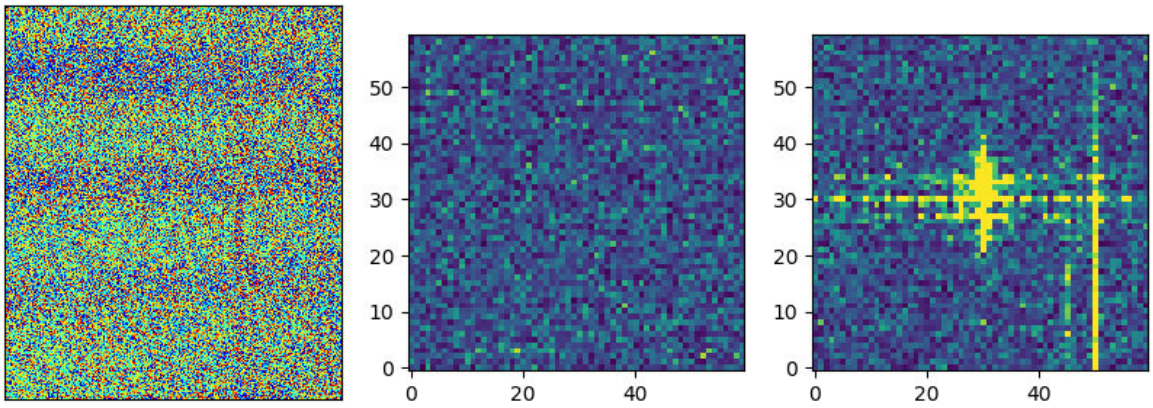

Figure 2: Dynamic closure phase spectrum on the triangle ST001-DE601-DE605 for the source 1327+5504 in the test field. Left: dynamic closure phase spectrum – note the source structure which causes averaging and decorrelation if the phases are simply averaged. Middle: Fourier transform of a random field of noise. Right: Fourier transform of the closure phase data.

Version 5 of the program is available from the github `nealjackson/lofar-lb`. There are unfortunately some non-backwards compatible changes:

- The main arguments are a list of measurement sets to process, and a list of closure triangles to examine. The latter are given in a string separated by semicolons (e.g. `'ST001;RS208;DE601;ST001;RS208;DE605'` examines two triangles between the superterp, RS208 and Effelsberg or Jülich). An `m` $\times$ `n` array is returned with `m` measurement sets and `n` triangles. The statistic issimply the sigma of the detection (note that random fields give sigmas of 1.5-2 because they are the maximum sigmas over a range of annuli).
- The arguments `doret`, `dopipe` and `doplot` have been removed. An argument `dump`

has been added; if `True`, a set of `m` × `n` .npy files will be written containing the dynamic spectra.

- The data are rearranged from the bizarre order given by CASAcore routines into strictly increasing frequency - i.e. the arrays returned have the spectral windows combined into a single SPW in which the channels increase monotonically. The routine will currently fail if the baselines do not have the same size in frequency or time. The arguments `bchan` and `echan` refer to the overall channels within the bandwidth, rather than in any one SPW.

- An argument `fromaips` has been added, because measurement sets written by AIPS store the antenna names in a different column of the MS.

The signal-to-noises produced on the same set of sources are as follows:

	DE601	DE602	DE603	DE604	DE605	FR606	SE607	UK608
1327+5504	136	60	143	126	266	48	58	38
1334+5501	7	2	5	2	22	3	2	0
1341+5344	1	2	3	2	3	1	4	1
1349+5341	33	11	24	29	66	20	21	17
1351+5518	9	3	5	1	24	0	3	2

It is interesting to note that DE605 is consistently higher S:N than DE601.

Finally, in Fig. 3 I show the transformed closure phases on three sources. Two of these

Conclusion. Version 5 of the closure phase coherence estimator includes a FFT step which produces the Fourier transform of the dynamic spectrum of the closure phase. This uses all of the information, and is virtually immune to the effects of delay miscalibration and source structure which the previous versions suffered from. It also provides a well-defined estimate of the significance of the detection. Finally it separates structure from confusing sources. It would be possible to use this technique to subtract confusing sources by Fourier filtering and re-transforming individual baselines, if they were reasonably well phase calibrated. It is also possible to see this as the basis for a way of doing imaging, or at least model-fitting.

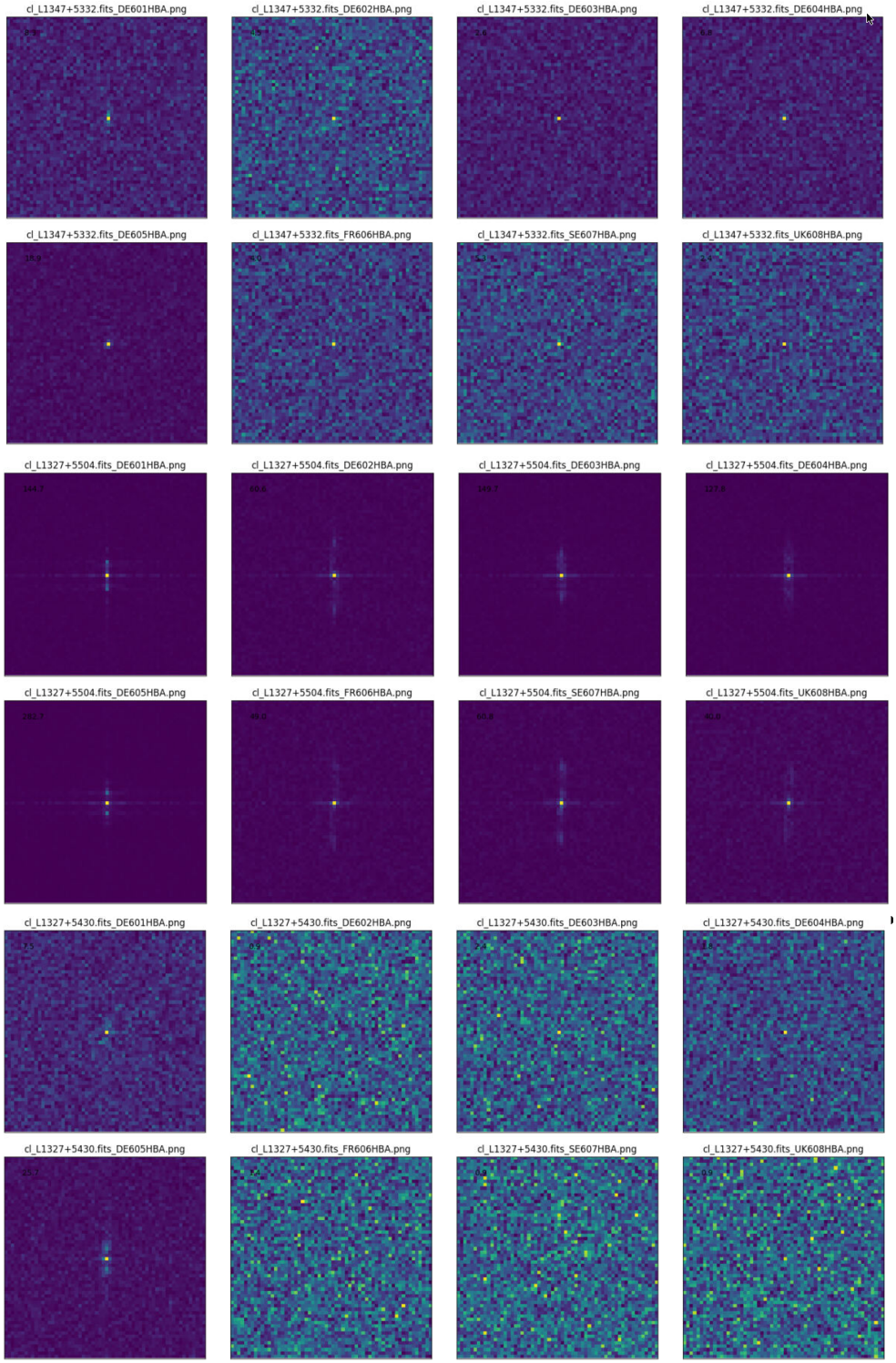

Figure 3: Transformed closure phase for three sources on all antennas. Note that extended structure is visible, and in principle an initial source model could be made using these images.